

AD-A060 983

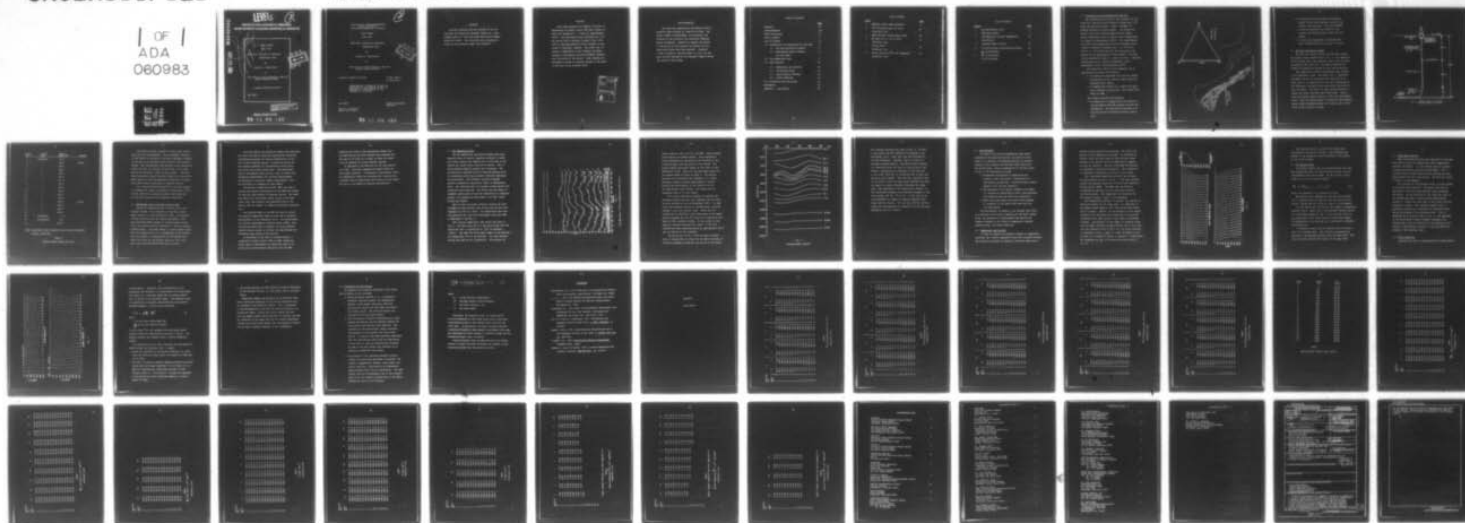
INSTITUTE FOR ACOUSTICAL RESEARCH MIAMI FLA
BEAR BUOY: ANALYSES OF ACQUIRED TEMPERATURE DATA.(U)
JUL 78 K L ECHTERNACHT
IAR-78001

F/G 20/1

N00014-74-C-0229
NL

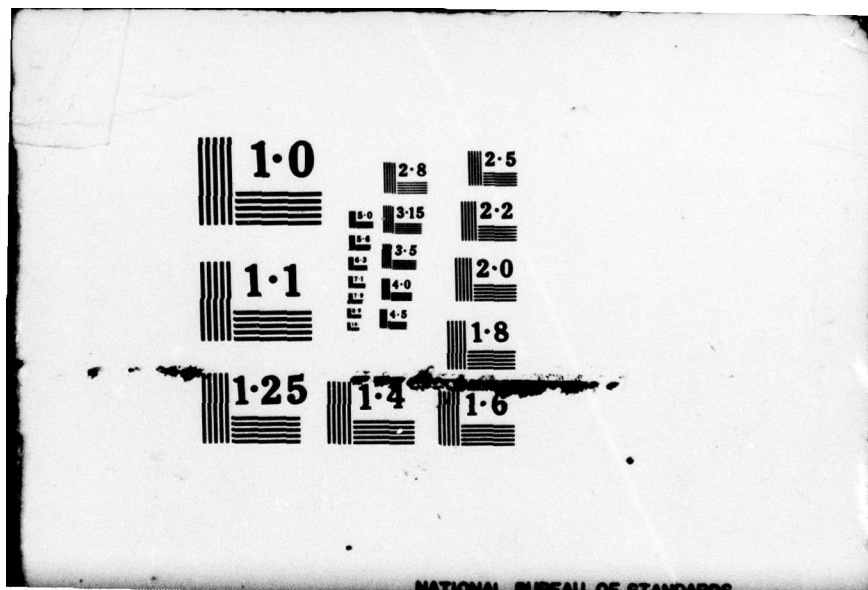
UNCLASSIFIED

1 OF 1
ADA
080983



END
DATE
FILMED

79
DDC



AD A060983

DDC FILE COPY

LEVEL

2_{SC}

**INSTITUTE FOR ACOUSTICAL RESEARCH
MIAMI DIVISION PALISADES GEOPHYSICAL INSTITUTE**

FINAL REPORT

July 1978

BEAR Buoy: Analyses of Acquired
Temperature Data

by

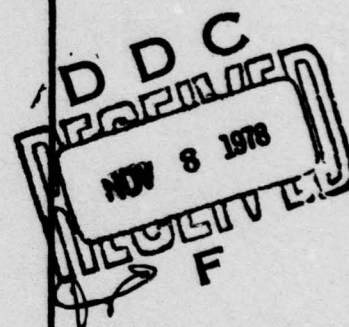
Kenneth L. Echternacht

to

The Office of Naval Research, Code 222
Sensor Systems Program

Contract N00014-74-C-0229

IAR 78001



This document has been approved
for public release and sale; its
distribution is unlimited.

Miami, Florida 33130

78 11 06 139

2

Institute for Acoustical Research
Miami Division of
Palisades Geophysical Institute

Final Report

July 1978

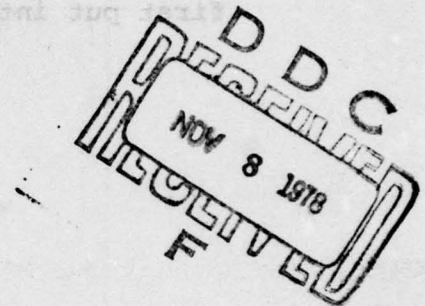
BEAR BUOY: Analyses of Acquired
Temperature Data

by

Kenneth L. Echternacht

to

The Office of Naval Research, Code 222
Sensor Systems Program



Contract: N00014-74-C-0229

14 May 1978 to
14 July 1978

"Reproduction in whole or in part is
permitted for any purpose of the U.S.
Government", Distribution of the
Document is Unlimited.

IAR 78001

Morton Kronengold,
Director

615 S.W. 2nd Avenue
Miami, Fla. 33130

78 11 06 139

NOTE

The work reported here was carried out at the Institute for Acoustical Research, Miami Div., from 8 March 1978 to 7 July 1978 under ONR Contract Number N00014-74-C-0229. "No inventions were conceived or first put into practice under this contract".

Abstract

This study examines the temporal variation in temperature at several levels from near surface to below the thermocline - a depth of approximately 1900 m. The time series were collected over a 51 day period from 16 February through 6 April 1976 from an area approximately 40 Km northeast of the island of Eleuthera, Bahamas. The study also includes an examination of the temporal and depth changes in the density and Brunt-Väisälä frequency over the period of the record. These changes are discussed in terms of observed changes in the level of activity of the internal tides.

ACCESSION for	
NTIS	White Section <input checked="" type="checkbox"/>
DDC	Buff Section <input type="checkbox"/>
UNANNOUNCED	<input type="checkbox"/>
JUSTIFICATION	
BY	
DISTRIBUTION/AVAILABILITY CODES	
Dist.	SPECIAL
A	

iii

Table of Contents

	<u>Page</u>
Abstract	ii
Acknowledgments	iii
Table of Contents	iv
List of Tables	v
List of Figures	vi
1.0 Introduction and Background For the Data	1
1.1 The Data Acquisition System	3
1.2 Methodology Used to Correct the Data Base	6
2.0 The Temperature Data	9
3.0 Data Analyses	14
3.1 Temperature and Salinity	14
3.2 The Density Field	17
3.3 Sound Velocity Profiles	18
3.4 Static Stability	18
4.0 Discussion and Conclusions	22
References	24
Appendix : Data Tables	25

List of Tables

<u>Table</u>		<u>Page</u>
1	Nominal Sensor Depth Locations	5
2	\bar{T} vs \bar{Z} Profile Data ($^{\circ}\text{C}$ vs m) (Profiles 1-25)	25
3	Mean Salinity Profile Data ($^{\circ}/\text{oo}$)	30
4	\bar{J}_t Data $(\text{g cm}^{-3}) \times 10^3$ (Profiles 1-25)	31
5	\bar{C} Data (ms^{-1}) (Profiles 1-25)	34
6	Static Stability $\bar{N}^2 \times 10^4$ ($\text{rad/sec})^2$ (Profiles 1-25)	37

List of Figures

<u>Figure</u>		<u>Page</u>
1	The Experimental Area	2
2	BEAR Buoy System	4
3	The BEAR Buoy 3-hourly Temperature Time Series	10
4	Isotherm Depth Location	12
5	\bar{T} vs \bar{Z} Profiles, Mean Salinity Profile	16
	$\bar{\sigma}_t$ vs \bar{Z} Profiles	
6	\bar{N}^2 vs \bar{Z} Profiles	19
	\bar{C} vs \bar{Z} Profiles	

1.0 Introduction and Background for the Data

The temperature data used in the analyses for this study were acquired during February through April 1976 using the BEAR Buoy System. (BEAR - acronym for Bermuda Eleuthera Acoustics Range). The system comprised a semi-taut surface buoyed mooring system using a thermistor cable to measure ocean temperatures to a depth of approximately 1900 m. The experimental site was located approximately 40 Km northeast of the island of Eleuthera, Bahamas (Fig. 1) at $25^{\circ} 45'N$, $76^{\circ} 17' W$. The anchor position was situated on the abyssal plain approximately 20 Km seaward of the base of the continental slope at a depth of 4797 m. Detailed descriptions can be found in Kronengold (1976), Echternacht (1976), and Echternacht (1977).

The scientific intent of the experiment was to provide data to study the following.

1. To examine the amplitude and relative changes in amplitude of the internal tides along the Eleuthera shelf region.
2. To compare the results of 1. above with open-ocean regions; in particular, the results from MODE and IWEX.

This report presents the following:

1. An examination of temperature time series at varying depths from near surface to below the thermocline. The time series represent a 51 day period from 16 February through 6 April, 1976.

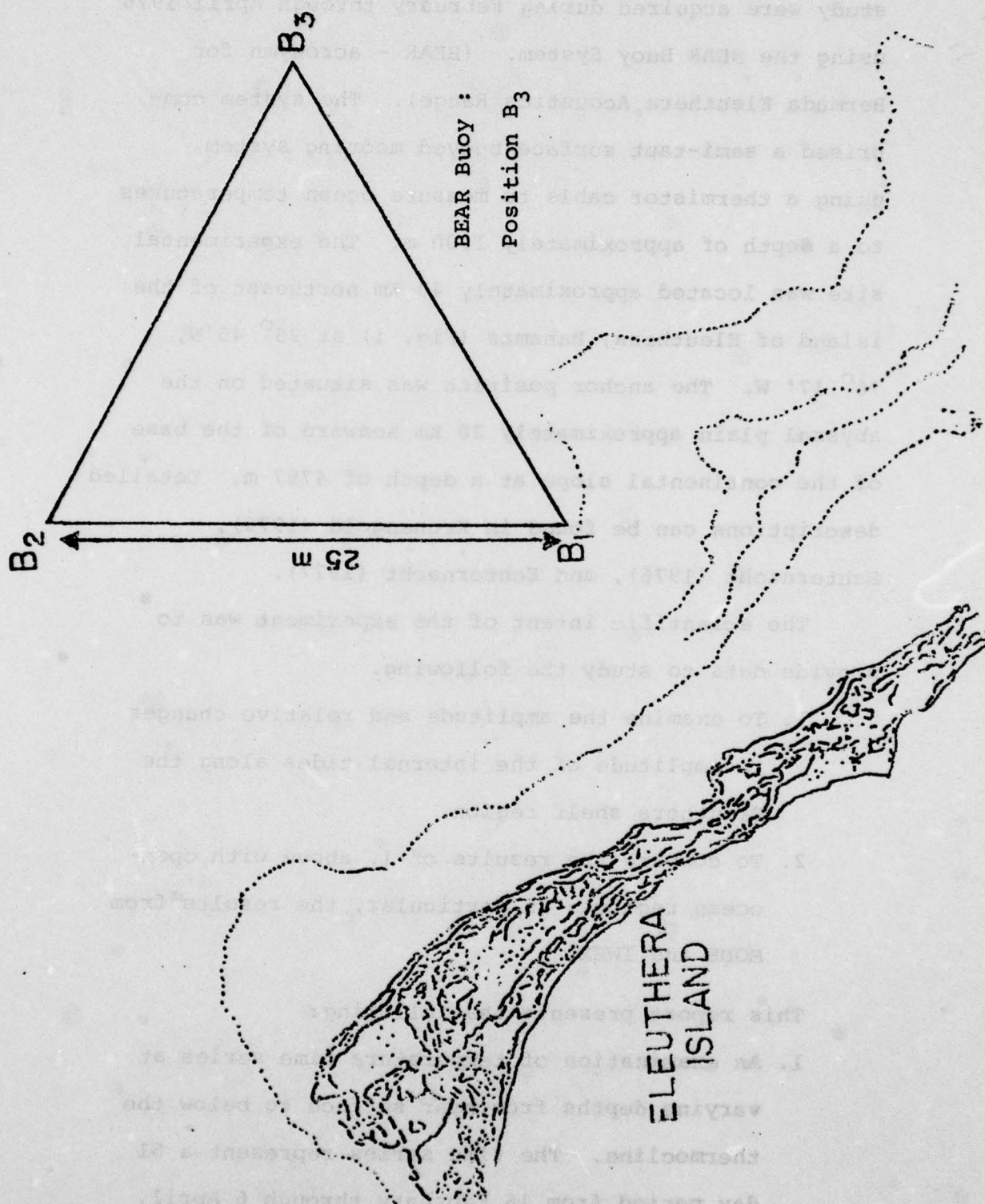


Fig. 1 The Experimental Area

2. An examination of both depth and temporal changes at the high frequency cutoff of the internal wave spectrum - the Brunt Väisälä.
3. A detailed discussion of changes in the internal semi-diurnal tidal field over this period.
4. A qualitative discussion of observed meso-scale features during the period of record.

1.1 The Data Acquisition System

The data were acquired using the BEAR Buoy system. The system, shown schematically in Fig. 2, was comprised of the surface buoy, the thermistor cable, and the nylon and ground tackle sections. The sensor subsystem included the temperature sensors and the mooring sensors.

The temperature sensors (thermistors) were encased in the thermistor cable. The cable, Fig. 2, comprised the upper portion of the mooring and consisted of an inner core of 37 conductors in a wet core configuration. The individual thermistor units were potted and spliced into the cable. The cable, in turn, was protected by a double lay torque balanced steel armor cable. Table 1 lists the nominal depth position of the individual sensor units. Here the nominal depth is defined as the reference sensor depth including mooring line stretch under conditions of zero external forcing.

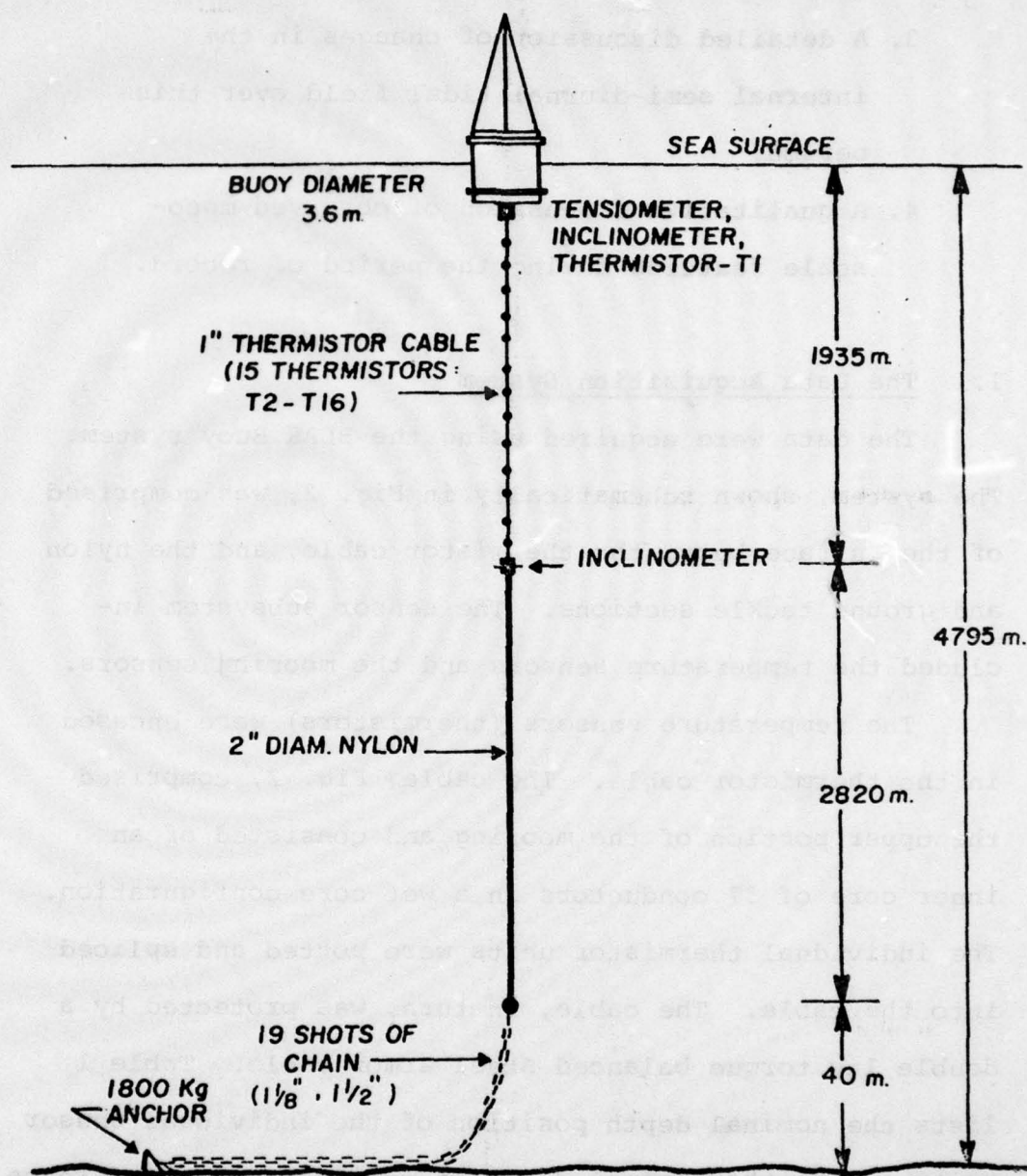


Fig. 2 BEAR BUOY SYSTEM

Sensor No.	Sensor Type	Nominal Depth (m)	Status
1	Thermistor	22.0	
2	"	148.9	non-op
3	"	249.4	
4	"	349.9	
5	"	450.4	
6	"	550.9	
7	"	651.3	
8	"	751.9	
9	"	852.4	
10	"	952.8	
11	"	1053.3	
12	"	1153.8	
13	"	1304.8	Non-op
14	"	1480.4	
15	"	1656.3	
16	"	1832.3	
17	Tensiometer	1.7 *	
18	Inclinometer	21.4	
19	"	1916.0	

*Note: Tensiometer depth measured from the mean waterline - nominal conditions

Table 1
Nominal Sensor Depth Locations

The mooring sensors included a strain gauge tensiometer and two inclinometers. The tensiometer, mounted in the clevis at the base of the buoy, provided a measure of the sum of the external forces acting on the mooring system. The inclinometers were mounted on the thermistor cable: one near the surface and the other at the lower end of the thermistor cable (~ 1900 m depth). The data from the mooring sensors provided inputs to an analytical model which was used to determine the mooring configuration under varying conditions of external forcing.

For a more detailed description of the data acquisition system the reader is referred to Echternacht (1976). In that study are included the design specifications for the buoy system and the component subsystems.

1.2 Methodology Used to Correct the Data Base

Before the temperature data could be used in any analysis scheme it was necessary to determine sensor depth locations at each acquisition time. As discussed in many previous works (eg, Wunsch and Dahlen, 1974) deep instrumentation located on surface buoyed mooring lines can undergo vertical excursions as large as several hundred meters. The large changes in sensor depth result from low frequency horizontal meanderings of the surface buoy and changes in configuration of the mooring line under the action of the surface forces of wind, wave, and current and subsurface drag due to current.

Given the above, two analytical models were developed. The first was used to study the generalities of mooring configuration changes for varying combinations of the above listed external forces. A second utilizing the same physics computed the environmental forces using explicitly the mooring sensor data. The methodology used in the general model and that used to correct the temperature measurements for vertical displacements are detailed in an earlier report (Echternacht, 1977). The following is a summary of those models.

The mooring configuration model (MCM) was used to analyze the mooring configuration of the BEAR Buoy system for specific case studies of external forcing. The model used explicitly the surface forces acting on the buoy (wind, wave, and current) and subsurface drag on the mooring (due to current) to compute the mooring configuration.

The modified model of the MCM was used to correct the acquired temperature data for bias due to vertical displacements of the thermistor units. The second model, the vertical displacement corrector model (VDCM), used the mooring sensor data to compute the total external surface forcing acting on the buoy and approximated the subsurface drag acting on the mooring.

As discussed in the above referenced report, a comparison of model results (MCM vs VDCM) showed the method used to approximate the subsurface drag to be valid and to yield results consistent with the MCM.

Comparison of VDCM vs XBT measurements showed that the VDCM reduced the error between buoy acquired and XBT data by as large as a factor of three for conditions of moderate to strong external forcing.

In application the VDCM was run for each acquisition time. The model computed the sensor depth for each sensor location. As detailed in Echternacht (1977) the temperature signal was corrected for vertical displacement bias by subtracting that portion of the signal due only to the change in mooring configuration.

2.0 The Temperature Data

The raw temperature and mooring sensors data were acquired using an interval sampling technique in which each sensor channel was sampled once at the rate of one channel per second during the turn-on period. The interval between sampling periods was 12 minutes. The raw data were converted from the acquired digital units to engineering units using transfer functions developed for each sensor. The transfer functions included specific calibration corrections (refer to Echternacht, 1976). The resulting data set yielded a times series with occasional data drop-outs. The latter was the result of equipment malfunctions during the acquisition or telemetry stages. For purposes of this study a 51.5 day "clean" section was chosen.

The 51.5 day (12 minute interval) section was then low-pass filtered yielding time series with the new high frequency cut off at 3 hours. The temperature data were then corrected for vertical displacement using the VDCM as discussed in Section 1.2.

The 3-hourly temperature time series are given in Fig. 3. The data cover the 51.5 day period from 1200 LST Julian Day (JD) 46 through JD 97, 1976 (15 February - 6 April). The axes are Julian Days (time) on the abscissa and temperature ($^{\circ}\text{C}$) on the ordinate. The same ordinate scaling was used for all thermistors. The records for

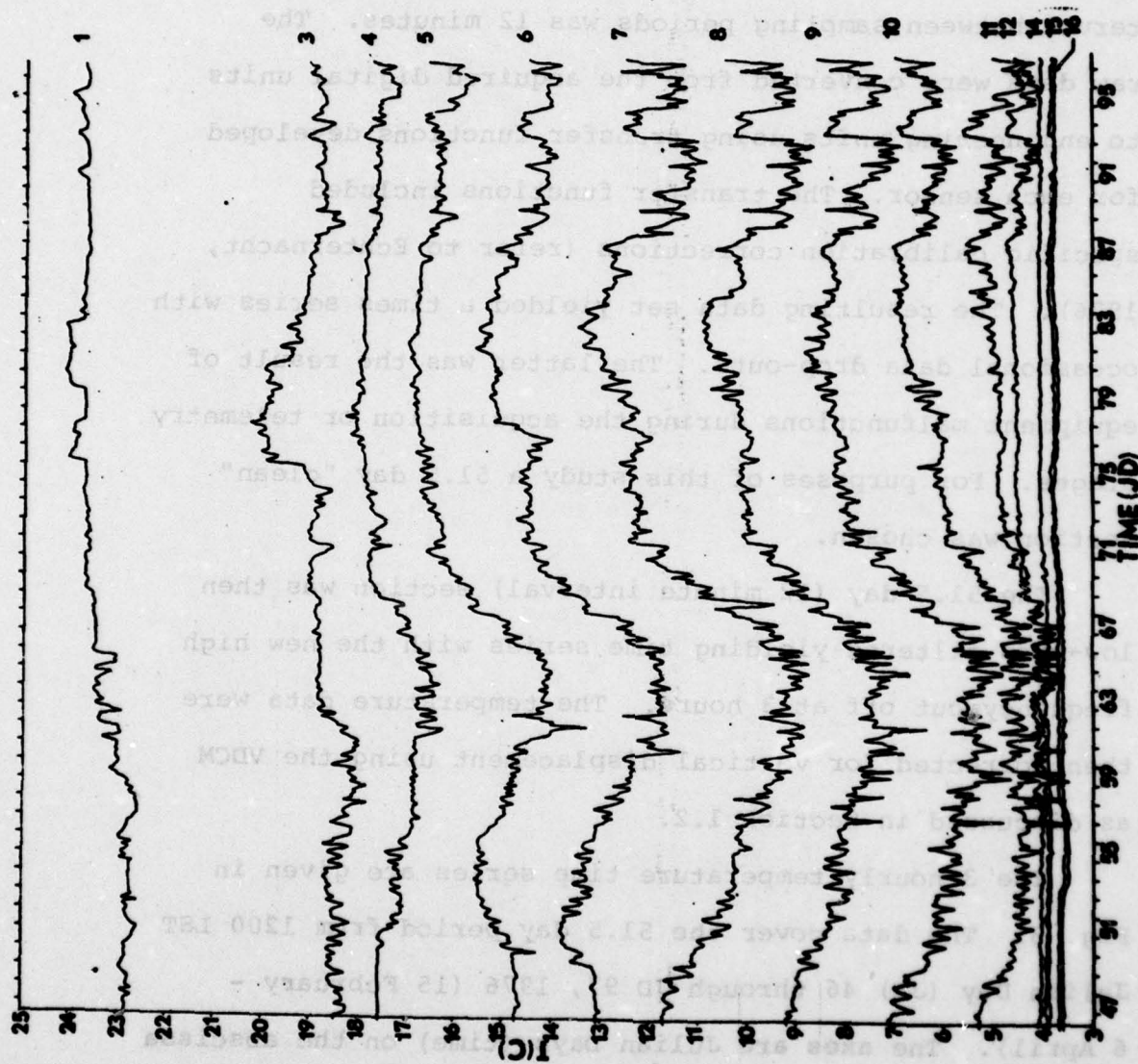


Fig. 3

The BEAR Buoy 3-hourly Temperature Time Series

sensor numbers 2 and 3 are not included - those sensors failed during the system implant. Each temperature trace represents the temperature that occurred at the corrected depth over the period of the record. The sensor numbers and depths appear to the right of each temperature trace. Here the corrected depth refers to the nominal depth as given in Table 1. The obvious features to be noted are the following: (1) a large mesoscale feature covering approximately a 24 day period from the beginning of the record to JD 70, (2) semi-diurnal oscillations. The latter will be discussed later on in this report.

For a first qualitative attempt to classify the mesoscale feature the data were compared with the Ring Criteria defined by Lai and Richardson (1977). In that study they examined changes in isotherm depth location through a cold core cyclonic eddy. Using the 15°C isotherm as an indicator it was noted that in the north-western Sargasso Sea the 15°C location is generally at a depth of 650 m outside an eddy. At the center of the eddy the following features are noted. (1) The 15°C isotherm has been displaced upward by approximately 500 m and (2) packing of the isotherms.

The data given in Fig. 3 were low-pass filtered using a running mean of 4 days and the depth location of selected isotherms plotted for the period of the record.

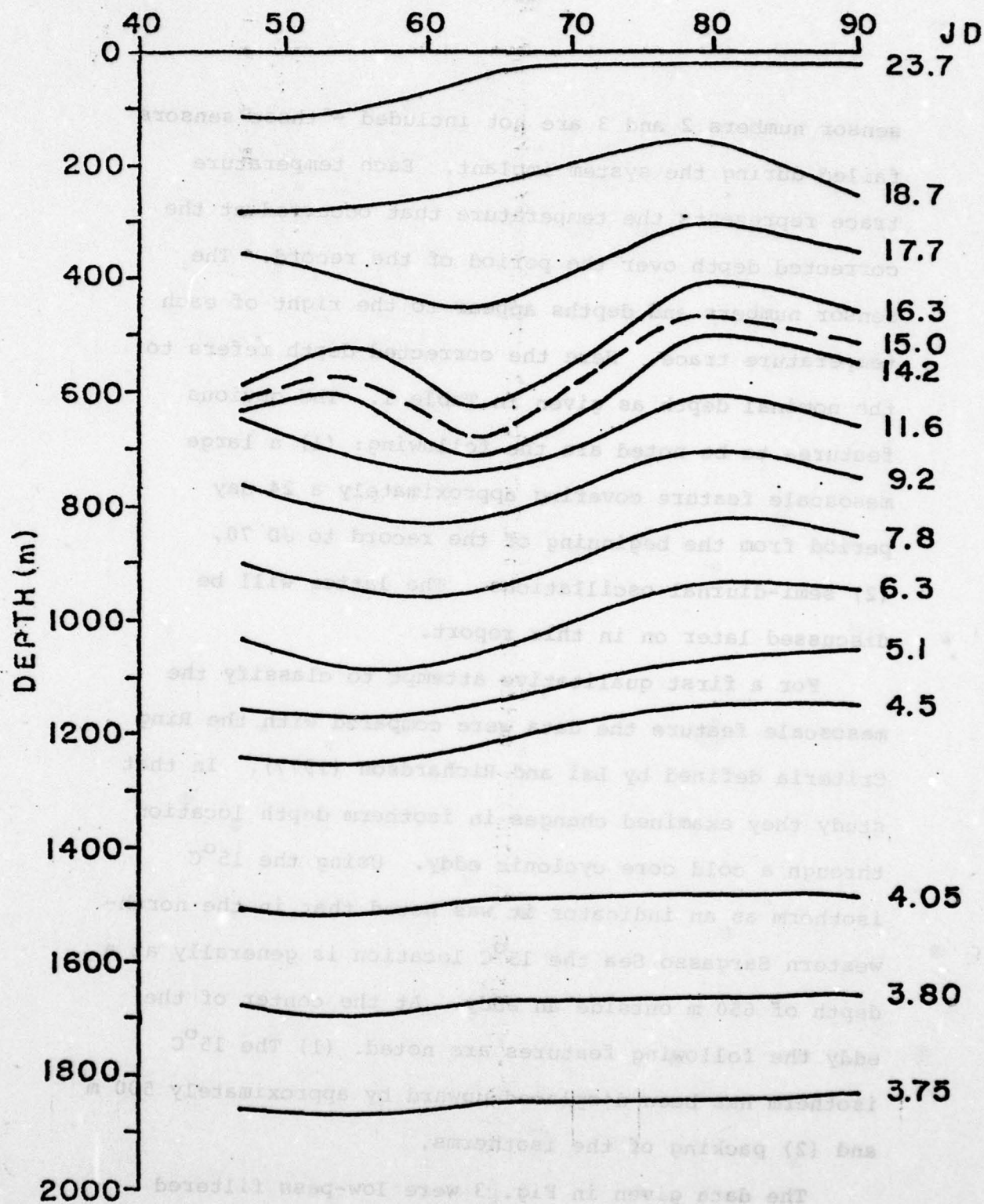


Fig. 4

Isotherm Depth Location

The isotherm locations are given in Fig. 4. As seen in the figure the 15°C isotherm is displaced by approximately 150 m - much less than that observed by Lai and Richardson. Secondly, there is little observable isotherm packing. The data present evidence of a mesoscale event but fail the ring criteria test. However, considering the proximity of the buoy site to the coast (~ 40 km) it is obvious that an eddy core would lie well seaward. Thus the only conclusion that can be drawn is that the event might possibly have been the edge of an eddy or meander traversing the study area. The importance of the observation, however, is that mesoscale features are relatively uncommon in the study region ($25^{\circ} 45'$, $76^{\circ} 17' \text{W}$). In the work by Lai and Richardson the number of sighted anomalies were broken down by regions. For the area $30-40^{\circ} \text{N}$, $60-80^{\circ} \text{W}$ there were 948 sightings as compared to 71 for the area bounded by $20-30^{\circ} \text{N}$, $65-80^{\circ} \text{W}$.

3.0 Data Analyses

In terms of the 3-hourly temperature time series presented in the previous section, the intent of this report is to provide a detailed description of and the changes in the internal semi-diurnal tidal field over the period shown. From an examination of the data given in Fig. 3, the following are noted.

- 1) Pronounced fluctuations in temperature are evident in the time series; fluctuations of a semi-diurnal periodicity. The semi-diurnal signal appears to be the most energetic.
- 2) The amplitude of the signal increases with depth to a maximum at approximately 1000 m then decreases with depth through and below the thermocline.
- 3) Within any given depth zone there exist changes in intensity of the signal with time over the 51.5 day period.

The distribution of energy in the internal wave field is a function of the static stability of the water column. Hence, the analyses to follow examine the spatial and temporal changes in the fields of temperature, density, sound velocity, and static stability.

3.1 Temperature and Salinity

In order to examine the temporal changes in temperature structure the 3-hourly temperature data were low-pass filtered. The filtering consisted of computing three-day means with a

one-day overlap between data sections. The filter was applied to the temperature data only. As discussed by Pickard (1964) for warm waters of low latitude origin changes in the density field are dominated by temperature not by salinity. Thus for this study the salinity is considered a conservative property. This assumption is reasonable considering the length of the record.

The 3-day mean temperature profiles and the mean salinity profile are given in Fig. 5. The mean salinity profile was obtained using data from the Fleet Numerical Weather Center (FNWC). The FNWC data are based on climatological XBT data for the study region during the winter months. The temperature and salinity data are listed in Tables 2 and 3 in the Appendix.

The temperature profiles, in general, are typical of the winter months for the study area. In comparison to the summer regime (Mooers, 1975) the shallow warm mixed layer is absent. However, at the beginning of the record (profiles 1-6) and during the latter half of the period (profiles 14-25) there exists a thin layer of decreased gradient. For profiles 1-6 the change in gradient occurs over the depth interval of approximately 250 to 550 m and over the interval of 250 to 650 m for the latter profiles. In reference to Fig. 4 (page 12) these correspond to the periods JD 47 through 59 and JD 74 through 97, respectively. The anomalies are due to the mesoscale feature seen in Fig. 4.

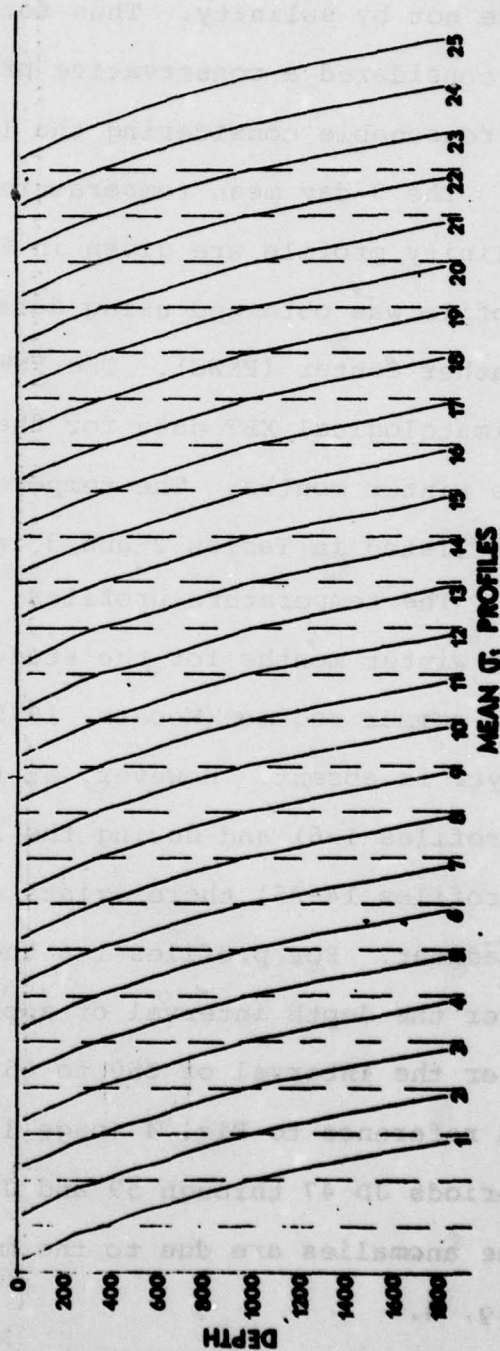
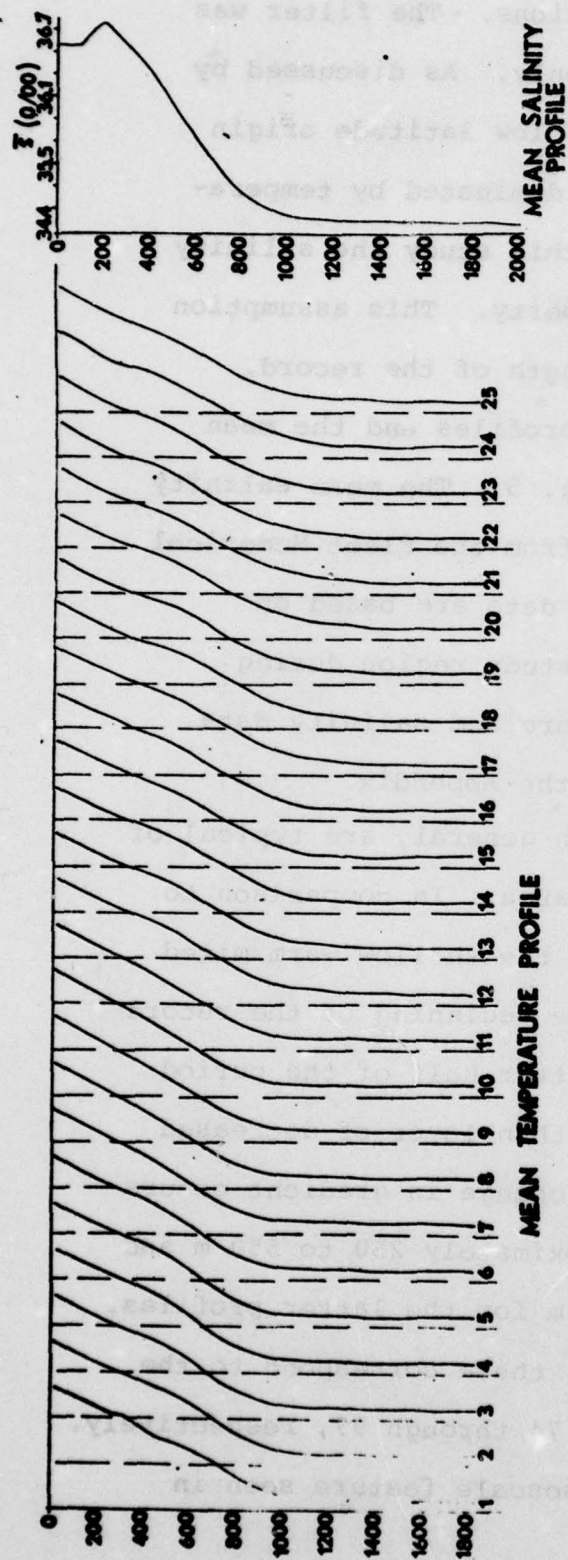


Fig. 5

The salinity profile is typical for those areas influenced by the Antilles Current. The characterizing feature is the subsurface salinity maximum in the region of 100 to 300 m depth.

3.2 The Density Field

The density anomaly, σ_t , was computed using the 3-day mean temperature data, the mean salinity profile, and the corresponding mean sensor depth. The σ_t as used in this study is the in situ density anomaly.

$$\sigma_t = (\rho_{s,t,p} - 1) \times 10^3 \quad (1)$$

where, the subscript s,t,p indicates in situ.

σ_t profiles were computed for each mean data section. Fig. 5 (bottom) gives the profiles over the period of the record. The σ_t data are listed in Table 4 in the Appendix.

In the case of the σ_t profiles the change in temperature gradient (Fig.5, upper) due to the mesoscale feature results in a noticeable anomaly in σ_t . As will be seen later in the discussion of the static stability these data suggest the possibility of an intrusion of a water mass of different characteristics.

It should be noted that the abscissa scale for Figs. 5 and 6 is a sliding scale. The vertical line separating profiles is the minimum abscissa value for each curve. The scale is given once for each figure in the upper left.

3.3 Sound Speed Profiles

Mean sound speed profiles were computed for each mean data section using the computed mean data (temperature, salinity, and depth). In the software used the pressure is obtained using the mean data listed above. Fig. 6 (bottom) gives the mean sound velocity profiles for each mean section over the 51-day period. The data are listed in Table 5 in the Appendix.

The influence of the mesoscale event is quite evident in the sound speed profiles. The depth level and the amplitude of the sound speed minimum change throughout the period. At the beginning of the record the level of the minimum decreases in depth through approximately profile 6. During the later half of the record the level increases in depth. This strongly suggests first a shallowing followed by a deepening of thermocline depth during the passage of the mesoscale event. This is supported by the results given in Fig. 4. The amplitude of the sound speed minimum increases throughout the period from a value of 1484 ms^{-1} at the beginning of the period to approximately 1488 ms^{-1} at the end after the passage of the mesoscale event.

3.4 Static Stability

Typically the ocean is characterized by stable density

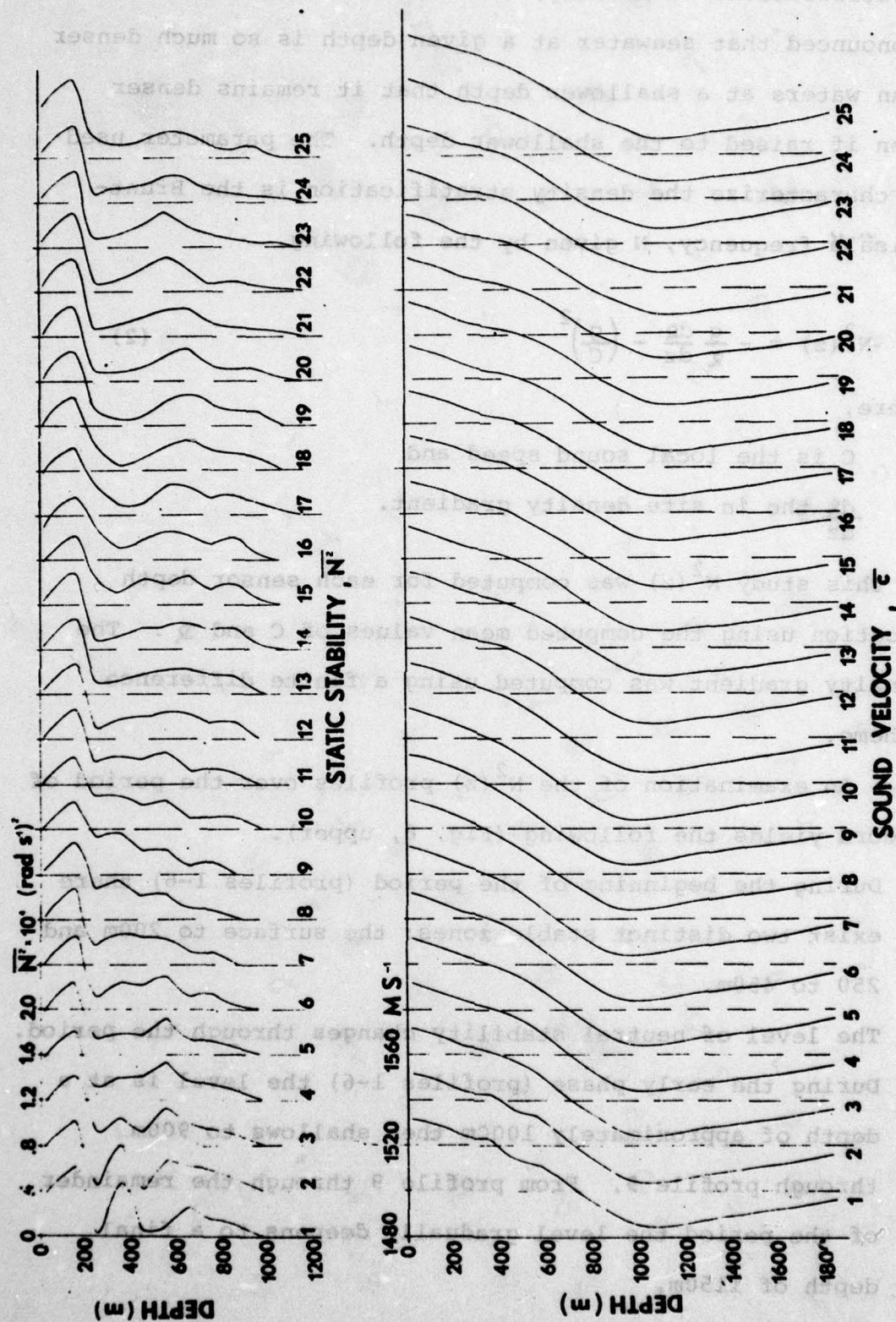


Fig. 6

stratification. Generally, the stratification is so pronounced that seawater at a given depth is so much denser than waters at a shallower depth that it remains denser even if raised to the shallower depth. The parameter used to characterize the density stratification is the Brunt-Väisälä frequency, N given by the following.

$$N^2(z) = -\frac{g}{\rho} \frac{d\rho}{dz} - \left(\frac{g}{C}\right)^2 \quad (2)$$

where,

C is the local sound speed and

$\frac{d\rho}{dz}$ the in situ density gradient.

In this study $N^2(z)$ was computed for each sensor depth location using the computed mean values of C and ρ . The density gradient was computed using a finite difference scheme.

An examination of the $N^2(z)$ profiles over the period of record yields the following (Fig. 6, upper).

1. During the beginning of the period (profiles 1-6) there exist two distinct stable zones: the surface to 200m and 250 to 450m.
2. The level of neutral stability changes through the period. During the early phase (profiles 1-6) the level is at a depth of approximately 1000m then shallows to 900m through profile 9. From profile 9 through the remainder of the period the level gradually deepens to a final depth of 1150m.

3. The latter profiles are more typical of waters influenced by the Antilles Current; ie, the stable zone at 100-300m depth.

These data suggest the presence of two distinct water masses during the beginning of the period associated with the passage of the mesoscale feature. This is supported by the perturbation in the level of neutral stability; ie, thermocline depth. During the earlier phases the fact that the deeper stable zone maintained its identity and that the character of the upper zone did not change appreciably through the record would suggest that the mesoscale feature did not have a surface signature of any consequence.

4.0 Discussion and Conclusions

To summarize the analyses presented in this study the following can be concluded.

1. During quiescent periods (i.e., no mesoscale transient features present) the temperature, density, sound speed, and static stability profiles are typical for the study area during the winter period. The profiles exhibit the influence of the Antilles Current.
2. Over the period of record fluctuations of a semi-diurnal periodicity are the dominant feature for time scales less than the local inertial. The intensity of the semi-diurnal signal, moreover, was observed to vary greatly over the 51-day period. In terms of the mode structure associated with the semi-diurnal wave field the implication of the above is that the distribution of energy by mode is variable rather than constant as is generally assumed for this region.
3. The passage of the transient mesoscale feature through the study area perturbed, noticeably, the fields of temperature, density, sound speed, and static stability - particularly at intermediate depths between 300 m and the thermocline. The mode shapes (vertical displacements due to the internal wave field) are directly proportional to the Brunt-Väisälä as given by the following.

$$\frac{d^2 Z_n}{dz^2} + \left(\frac{N^2 - \sigma^2}{\sigma^2 - f^2} \right) \alpha_n^2 Z_n = 0 \quad (3)$$

where,

Z_n is the vertical displacement,

σ the semi-diurnal tidal frequency,

f the local inertial, and

α the wave number.

Obviously, the solution to Eq. (3) using the N^2 profiles presented in this study would yield a much more complicated picture of the internal wave field for the study area. In particular, the modal structure and distribution of energy by mode changes considerably with time. The importance of these findings to acoustics study for the Bermuda-Eleuthera range is obvious.

Future analyses using the BEAR Buoy data set should examine in detail the modal structure and changes in distribution by mode over the period or record.

REFERENCES

- Echternacht, K.L., 1976: BEAR Buoy: The engineering documentation for scientific application. IAR Report No. 76002.
- _____, 1977: The mooring configuration model and method used to correct sensors for vertical displacements. IAR Report No. 77008.
- Kronengold, M., 1976: BEAR: An environmental measurement buoy. Proceedings of the 22nd Internat. Instrumentation Symposium, San Diego, Cal., May 25-27, 1976.
- Lai, D.Y. and P.L. Richardson, 1977: Distribution and movement of Gulf Stream rings. J. Phys. Oceanogr., 7, 670-683.
- Mooers, C.N.K., 1975: Sound-velocity perturbations due to low-frequency motions in the ocean. J. Acoust. Soc. Am., 57, 1067-1075.
- Pickard, G.L., 1964: Descriptive Physical Oceanography. Pergamon Press, 199pp.
- Wunsch, C. and J.M. Dahlen, 1974: A moored temperature and pressure recorder. Deep-Sea Res., 21, 145-154.

Appendix:

Data Tables

Profile No.	1		2		3		4		5	
	T	Z	T	Z	T	Z	T	Z	T	Z
1	22.8	22.0	22.8	22.0	22.8	22.0	22.8	22.1	22.8	22.1
2	20.4	150.0	20.4	150.0	20.4	150.0	20.4	150.0	20.3	150.0
3	18.5	249.6	18.5	249.6	18.5	249.6	18.5	249.6	18.3	249.7
4	17.6	350.2	17.5	350.2	17.2	350.2	17.2	350.2	16.9	350.3
5	14.7	450.7	14.9	450.7	15.3	450.7	15.5	450.7	15.2	450.8
6	13.2	551.3	13.6	551.3	13.5	551.3	13.3	551.3	13.1	551.4
7	11.4	651.8	10.9	651.8	10.5	651.8	10.2	651.9	10.0	652.0
8	8.9	752.4	8.6	752.4	8.2	752.4	8.1	752.4	8.0	752.6
9	6.7	852.9	6.2	852.9	6.0	852.9	5.9	853.0	5.8	853.2
10	5.0	953.5	4.6	953.5	4.4	953.5	4.4	953.5	4.4	953.8
11	4.0	1054.0	4.0	1054.0	4.0	1054.0	4.0	1054.1	4.0	1054.3
12	3.9	1154.6	3.9	1154.6	3.9	1154.6	3.9	1154.7	3.9	1154.9
13	3.9	1481.4	3.9	1481.4	3.9	1481.4	3.8	1481.5	3.8	1481.8
14	3.7	1657.4	3.7	1657.4	3.7	1657.4	3.6	1657.5	3.6	1657.8
15	3.6	1833.4	3.6	1833.3	3.6	1833.4	3.5	1833.4	3.5	1833.9

Table

 \bar{T} vs \bar{Z} Profile Data ($^{\circ}\text{C}$ vs m)

(Profiles 1-25)

Profile No.	6		7		8		9		10	
Data No.	T	Z	T	Z	T	Z	T	Z	T	Z
1	22.8	22.1	23.0	22.1	23.3	22.1	23.4	22.1	23.4	22.1
2	20.2	150.0	20.3	150.0	20.6	150.0	20.8	150.0	20.8	150.0
3	18.1	249.8	18.2	249.8	18.5	249.6	18.8	249.9	18.8	250.0
4	16.8	350.5	16.7	350.4	16.6	350.2	16.6	350.5	16.8	350.7
5	14.9	451.1	14.6	451.1	14.2	450.8	14.1	451.2	14.6	451.4
6	12.6	551.8	12.1	551.7	11.9	551.3	11.8	551.8	12.2	552.1
7	9.6	652.4	9.3	652.3	9.2	651.9	9.1	652.5	9.4	652.8
8	7.7	753.0	7.4	752.9	7.3	752.5	7.4	753.1	7.6	753.5
9	5.5	853.7	5.3	853.6	5.4	853.0	5.3	853.8	5.5	854.2
10	4.3	954.3	4.5	954.2	4.5	953.6	4.5	954.4	4.5	954.9
11	4.0	1055.0	4.0	1054.8	4.1	1054.2	4.0	1055.1	4.0	1055.5
12	3.9	1155.6	3.9	1155.4	4.0	1154.7	3.9	1155.7	3.9	1156.2
13	3.8	1482.7	3.9	1482.5	3.9	1481.6	3.9	1482.8	3.9	1483.5
14	3.6	1658.8	3.7	1658.6	3.7	1657.6	3.7	1659.9	3.7	1659.7
15	3.6	1834.9	3.6	1834.6	3.6	1833.5	3.6	1835.1	3.6	1835.9

Table

\bar{T} vs \bar{Z} Profile Data ($^{\circ}\text{C}$ vs m)
(Profiles 1-25)

Profile No.	11		12		13		14		15	
Data No.	T	Z	T	Z	T	Z	T	Z	T	Z
1	23.6	22.1	23.7	22.1	23.7	22.0	23.7	22.0	23.8	22.0
2	21.1	150.0	21.1	150.0	21.1	150.0	21.1	150.0	21.4	150.0
3	18.9	249.9	18.9	249.7	18.9	249.6	18.9	249.5	19.6	249.6
4	17.3	350.6	17.7	350.3	17.6	350.1	17.8	350.0	17.9	350.1
5	15.4	451.2	16.1	450.8	16.3	450.7	16.5	450.6	16.6	450.7
6	13.1	551.9	14.0	551.4	14.4	551.2	14.5	551.1	14.4	551.2
7	10.3	652.6	11.5	652.0	12.1	651.7	12.3	651.6	12.3	651.8
8	8.4	753.2	9.2	752.6	9.9	752.3	10.1	752.1	10.0	752.3
9	6.3	853.9	7.1	853.2	7.7	852.8	8.0	852.6	8.1	852.8
10	4.8	954.5	5.3	953.8	5.8	953.4	6.0	953.2	6.1	953.4
11	4.2	1055.2	4.5	1054.3	4.7	1053.9	4.8	1053.7	4.8	1053.9
12	4.1	1155.9	4.4	1154.9	4.5	1154.4	4.5	1154.2	4.5	1154.5
13	3.9	1483.0	4.0	1481.8	4.0	1481.2	4.0	1480.9	4.0	1481.2
14	3.7	1659.2	3.7	1657.8	3.8	1657.1	3.8	1656.8	3.8	1657.2
15	3.6	1835.3	3.7	1833.8	3.7	1833.1	3.8	1832.7	3.7	1833.1

Table

 \bar{T} vs \bar{Z} Profile Data ($^{\circ}\text{C}$ vs m)

(Profiles 1-25)

Profile No.	16		17		18		19		20	
	T	Z	T	Z	T	Z	T	Z	T	Z
1	23.8	22.1	23.9	22.1	24.0	22.1	23.8	22.1	23.7	22.1
2	21.7	150.0	21.4	150.0	21.5	150.0	21.2	150.0	21.1	150.0
3	20.0	249.9	19.8	249.9	19.5	249.8	19.2	249.7	19.0	249.8
4	18.1	350.5	18.0	350.5	17.9	350.4	17.9	350.3	17.9	350.4
5	16.8	451.1	16.8	451.1	16.9	451.0	16.8	450.9	16.7	451.0
6	14.8	551.8	15.2	551.8	15.3	551.6	15.3	551.5	15.0	551.6
7	12.3	652.4	12.7	652.4	13.1	652.2	13.0	652.1	12.7	652.2
8	10.1	753.0	10.4	753.1	10.7	752.8	10.6	752.7	10.2	752.8
9	8.2	853.7	8.4	853.7	8.5	853.4	8.4	853.2	8.3	853.4
10	6.1	954.3	6.5	954.3	6.7	954.0	6.8	953.8	6.8	954.0
11	4.8	1054.9	4.9	1055.0	5.0	1054.6	5.1	1054.4	5.2	1054.6
12	4.5	1155.6	4.5	1155.6	4.5	1155.2	4.6	1155.0	4.6	1155.3
13	4.0	1482.7	4.0	1482.7	4.0	1482.2	4.0	1481.9	4.1	1482.2
14	3.8	1658.8	3.8	1658.8	3.8	1658.2	3.8	1657.9	3.9	1658.3
15	3.7	1834.9	3.7	1834.9	3.7	1834.3	3.8	1834.0	3.8	1834.4

Table

 \bar{T} vs \bar{Z} Profile Data ($^{\circ}\text{C}$ vs m)

(Profiles 1-25)

Profile No.	21		22		23		24		25	
	T	Z	T	Z	T	Z	T	Z	T	Z
1	23.7	22.1	23.7	22.1	23.7	22.2	23.8	22.2	23.8	22.1
2	21.0	150.0	20.9	150.0	21.0	150.0	21.1	150.0	21.1	150.0
3	18.8	249.7	18.7	249.7	18.8	250.1	18.7	250.2	18.9	250.0
4	17.8	350.3	17.6	350.3	17.7	350.8	17.7	350.9	17.4	350.7
5	16.5	450.9	16.3	451.0	16.3	451.5	16.3	451.7	16.0	451.4
6	14.6	551.5	14.2	551.6	14.2	552.3	14.4	552.5	14.1	552.1
7	12.2	652.1	11.4	652.2	11.3	653.0	11.9	653.2	11.7	652.8
8	9.9	752.7	9.2	752.8	9.2	753.7	9.7	754.0	9.5	753.5
9	8.0	853.3	7.6	853.4	7.4	854.4	7.8	854.7	7.6	854.2
10	6.6	953.9	6.2	954.0	6.1	955.2	6.4	955.5	6.4	954.9
11	5.2	1054.5	5.0	1054.6	5.0	1055.9	5.1	1056.2	4.7	1055.6
12	4.5	1155.1	4.4	1155.2	4.3	1156.6	4.4	1157.0	4.3	1156.3
13	4.1	1482.1	4.0	1482.1	4.0	1484.0	4.0	1484.4	4.0	1483.5
14	3.8	1658.1	3.8	1658.2	3.8	1660.2	3.8	1660.8	3.8	1659.7
15	3.8	1834.2	3.8	1834.2	3.8	1836.5	3.8	1837.1	3.8	1836.0

Table

\bar{T} vs \bar{Z} Profile Data ($^{\circ}\text{C}$ vs m)
(Profiles 1-25)

Data No.	Depth (m)	\bar{S} (o/oo)
1	0	36.54
2	100	36.54
3	200	36.74
4	300	36.55
5	400	36.34
6	500	36.04
7	600	35.75
8	700	35.50
9	800	35.24
10	900	35.14
11	1000	35.03
12	1100	35.02
13	1200	35.02
14	1300	35.01
15	1400	35.01
16	1500	35.01
17	1600	34.99
18	1700	34.98
19	1800	34.97
20	1900	34.96
21	2000	34.95

Table

Mean Salinity Profile Data (o/oo)

Profile
No.

Data No.	1	2	3	4	5	6	7	8	9	10
1	25.23	25.23	25.23	25.23	25.23	25.23	25.17	25.08	25.06	25.06
2	26.29	26.29	26.29	26.29	26.32	26.34	26.30	26.22	26.17	26.17
3	27.36	27.36	27.36	27.36	27.41	27.46	27.43	27.36	27.28	27.28
4	27.82	27.85	27.92	27.92	27.99	28.02	28.04	28.07	28.07	28.02
5	28.75	28.70	28.61	28.57	28.64	28.71	28.77	28.86	28.88	28.77
6	29.24	29.16	29.18	29.22	29.26	29.37	29.47	29.51	29.54	29.46
7	29.78	29.88	29.96	30.01	30.05	30.12	30.18	30.19	30.21	30.16
8	30.50	30.55	30.62	30.62	30.65	30.70	30.75	30.76	30.75	30.72
9	31.11	31.19	31.22	31.23	31.25	31.29	31.32	31.30	31.32	31.29
10	31.69	31.74	31.77	31.77	31.77	31.79	31.76	31.76	31.76	31.76
11	32.16	32.16	32.16	32.16	32.16	32.16	32.16	32.14	32.16	32.16
12	32.58	32.58	32.58	32.58	32.58	32.58	32.58	32.57	32.58	32.59
13	33.91	33.91	33.91	33.92	33.92	33.93	33.91	33.91	33.91	33.92
14	34.65	34.65	34.65	34.66	34.66	34.67	34.65	34.65	34.65	34.66
15	35.37	35.37	35.37	35.39	35.39	35.38	35.38	35.37	35.38	35.38

Table
Data ($Q-1$) $\times 10^3$ (gcm^{-3})
(Profiles 1-25)

Profile
No.

Data No.	11	12	13	14	15	16	17	18	19	20
1	25.00	24.94	24.97	24.97	24.94	24.94	24.91	24.88	24.94	24.97
2	26.12	26.11	26.11	26.11	26.00	25.95	25.96	25.99	26.06	26.10
3	27.25	27.25	27.25	27.25	27.07	26.96	27.02	27.10	27.18	27.23
4	27.90	27.80	27.82	27.77	27.75	27.70	27.72	27.75	27.75	27.75
5	28.59	28.43	28.38	28.33	28.31	28.26	28.26	28.23	28.26	28.28
6	29.27	29.07	28.98	28.96	28.98	28.89	28.80	28.78	28.78	28.85
7	30.00	29.76	29.64	29.60	29.60	29.60	29.52	29.43	29.45	29.52
8	30.58	30.44	30.31	30.28	30.30	30.28	30.22	30.16	30.18	30.26
9	31.18	31.05	30.95	30.90	30.88	30.87	30.83	30.82	30.83	30.85
10	31.72	31.65	31.58	31.54	31.53	31.53	31.47	31.44	31.42	31.42
11	32.14	32.09	32.06	32.05	32.05	32.05	32.04	32.02	32.01	32.00
12	32.56	32.52	32.50	32.50	32.50	32.50	32.50	32.50	32.49	32.49
13	33.92	33.90	33.89	33.89	33.89	33.90	33.90	33.90	33.90	33.88
14	34.66	34.65	34.63	34.63	34.63	34.64	34.64	34.65	34.64	34.62
15	35.38	35.36	35.36	35.34	35.36	35.36	35.36	35.36	35.34	35.35

Table

$\bar{\sigma}_t$ Data (Q-1) $\times 10^3$ (gcm⁻³)

(Profiles 1-25)

Profile
No.

Data
No.

	21	22	23	24	25
1	24.97	24.97	24.97	24.94	24.94
2	26.12	26.14	26.12	26.11	26.10
3	27.28	27.30	27.28	27.28	27.26
4	27.77	27.82	27.80	27.80	27.87
5	28.33	28.38	28.38	28.38	28.45
6	28.94	29.03	29.03	28.99	29.05
7	29.62	29.78	29.80	29.69	29.72
8	30.32	30.44	30.45	30.36	30.39
9	30.90	30.97	31.00	30.94	30.97
10	31.46	31.52	31.54	31.49	31.49
11	32.00	32.02	32.03	32.02	32.07
12	32.50	32.52	32.54	32.52	32.53
13	33.88	33.90	33.90	33.91	33.90
14	34.64	34.64	34.64	34.65	34.64
15	35.35	35.35	35.36	35.36	35.35

Table

$\bar{\sigma}_t$ Data (R-1) $\times 10^3$ (gcm⁻³)

(Profiles 1-25)

Profile
No.

Data No.	1	2	3	4	5	6	7	8	9	10
1	1531.6	1531.6	1531.6	1531.6	1531.6	1531.6	1532.0	1532.8	1533.0	1533.0
2	1527.8	1527.7	1527.7	1527.7	1527.5	1527.2	1527.6	1528.4	1528.9	1528.9
3	1523.9	1523.9	1523.9	1523.9	1523.4	1522.8	1523.1	1523.9	1524.8	1524.9
4	1522.8	1522.5	1521.6	1521.6	1520.7	1520.4	1520.1	1519.8	1519.8	1520.4
5	1515.3	1515.9	1517.2	1517.8	1516.9	1515.9	1515.0	1513.7	1513.4	1515.0
6	1511.7	1513.0	1512.7	1512.0	1511.4	1509.7	1508.0	1507.3	1507.0	1508.3
7	1506.8	1505.1	1503.6	1502.6	1501.9	1500.4	1499.3	1498.9	1498.6	1500.0
8	1499.2	1498.1	1496.6	1496.2	1495.8	1494.7	1493.5	1493.1	1493.5	1494.3
9	1492.2	1490.2	1489.4	1489.0	1488.6	1487.4	1486.6	1487.0	1486.6	1487.4
10	1486.9	1485.2	1484.4	1484.4	1484.4	1484.0	1484.8	1484.8	1484.8	1484.8
11	1484.3	1484.3	1484.3	1484.3	1484.3	1484.3	1484.3	1484.7	1484.3	1484.3
12	1485.5	1485.5	1485.5	1485.5	1485.5	1485.6	1485.6	1486.0	1485.6	1485.6
13	1491.0	1491.0	1491.0	1490.6	1490.6	1490.6	1491.0	1491.0	1491.0	1491.0
14	1493.1	1493.1	1493.1	1492.7	1492.7	1492.7	1493.2	1493.2	1493.2	1493.2
15	1495.7	1495.7	1495.7	1495.3	1495.3	1495.7	1495.7	1495.7	1495.7	1495.7

Table

\bar{C} Data (ms^{-1})

(Profiles 1-25)

Profile
No.

Data No	11	12	13	14	15	16	17	18	19	20
1	1533.5	1533.8	1533.8	1533.8	1534.0	1534.0	1534.2	1534.5	1534.0	1533.8
2	1529.3	1529.4	1529.4	1529.4	1530.5	1531.1	1530.9	1530.6	1530.0	1529.6
3	1525.1	1525.1	1525.1	1525.1	1527.0	1528.1	1527.6	1526.7	1525.9	1525.4
4	1521.9	1523.0	1522.8	1523.3	1523.6	1524.2	1523.9	1523.6	1523.6	1523.6
5	1517.5	1519.7	1520.3	1520.9	1521.2	1521.8	1521.8	1522.1	1521.8	1521.5
6	1511.4	1514.3	1515.6	1515.9	1515.6	1516.9	1518.2	1518.5	1518.5	1517.5
7	1503.0	1507.2	1509.3	1509.9	1509.9	1510.0	1511.3	1512.6	1512.3	1511.3
8	1497.3	1500.3	1502.9	1503.6	1503.2	1503.6	1504.7	1505.8	1505.4	1504.0
9	1490.6	1493.7	1496.1	1497.2	1497.6	1498.0	1498.7	1499.1	1498.7	1498.4
10	1486.1	1488.1	1490.1	1490.9	1491.3	1491.3	1492.9	1493.7	1494.1	1494.1
11	1485.1	1486.4	1487.2	1487.6	1487.6	1487.6	1488.0	1488.4	1488.8	1489.2
12	1486.4	1487.6	1488.0	1488.0	1488.0	1488.0	1488.0	1488.0	1488.4	1488.5
13	1491.0	1491.4	1491.4	1491.4	1491.4	1491.4	1491.4	1491.4	1491.4	1491.9
14	1493.2	1493.1	1493.6	1493.6	1493.6	1493.6	1493.6	1493.6	1493.6	1494.0
15	1495.7	1496.1	1496.1	1496.5	1496.1	1496.1	1496.1	1496.1	1496.5	1496.5

Table

\bar{C} Data (ms^{-1})
(Profiles 1-25)

Profile
No.

Data
No.

21

22

23

24

25

1	1533.8	1533.8	1533.8	1534.0	1534.0
2	1529.3	1529.1	1529.3	1529.4	1529.5
3	1524.8	1524.5	1524.8	1524.8	1525.1
4	1523.3	1522.8	1523.0	1523.0	1522.2
5	1520.9	1520.3	1520.3	1520.3	1519.4
6	1516.3	1515.0	1515.0	1515.6	1514.7
7	1509.6	1507.8	1506.5	1508.6	1507.9
8	1502.9	1500.3	1500.3	1502.2	1501.4
9	1497.2	1495.7	1494.9	1496.5	1495.7
10	1493.3	1491.7	1491.4	1492.6	1492.5
11	1489.2	1488.4	1488.4	1488.9	1487.2
12	1488.0	1487.6	1487.2	1487.7	1487.2
13	1491.9	1491.4	1491.5	1491.5	1491.5
14	1493.6	1493.6	1493.6	1493.6	1493.6
15	1496.5	1496.5	1496.6	1496.6	1496.6

Table

\bar{C} Data (ms^{-1})

(Profiles 1-25)

Profile No.	1	2	3	4	5	6	7	8	9	10
1	3.84	3.84	3.84	3.84	4.04	4.22	4.35	4.39	4.22	4.22
2	6.07	6.07	6.07	6.07	6.30	6.53	6.69	6.77	6.52	6.51
3	0.28	0.51	1.21	1.21	1.42	1.17	1.64	2.59	3.33	2.87
4	4.65	3.98	2.41	1.97	1.93	2.34	2.75	3.37	3.57	2.98
5	0.50	0.12	1.19	2.04	1.78	2.12	2.45	1.98	1.96	2.25
6	0.88	2.63	3.15	3.27	3.21	2.90	2.43	2.21	2.18	2.45
7	2.52	2.08	1.99	1.61	1.42	1.18	1.13	1.11	0.79	0.99
8	1.53	1.76	1.38	1.36	1.34	1.27	1.07	0.78	1.07	1.11
9	1.17	0.95	0.92	0.78	0.64	0.35				0.10
10	0.07									

*Note: Blanks indicate the data approach 0.0

Table
 $\overline{N^2} \times 10^4 \text{ (rad/sec)}^2$
 (Profiles 1-25)

Profile
No.

Data No.	11	12	13	14	15	16	17	18	19	20
1	4.35	4.46	4.45	4.45	3.88	3.49	3.80	4.21	4.28	4.36
2	6.68	6.84	6.85	6.86	6.12	5.59	5.98	6.51	6.61	6.70
3	1.96	1.02	1.26	0.79	2.30	2.83	2.56	2.04	1.29	0.79
4	2.42	1.82	1.13	1.15	1.16	1.18	0.94	0.47	0.70	0.93
5	2.22	1.95	1.56	1.81	2.25	1.86	0.99	1.01	0.77	1.20
6	2.68	2.35	2.05	1.88	1.66	2.52	2.61	2.03	2.23	2.17
7	1.31	2.21	2.16	2.20	2.38	2.20	2.45	2.72	2.70	2.81
8	1.28	1.44	1.75	1.63	1.29	1.30	1.52	1.91	1.89	1.32
9	0.84	1.38	1.56	1.82	1.84	2.00	1.76	1.62	1.31	1.14
10			0.33	0.44	0.58	0.58	1.04	1.21	1.22	1.09
11							0.43	0.18	0.18	0.32

Table

*Note: Blanks indicate the data approach 0.0

Static Stability $\overline{N^2} \times 10^4$ (rad/sec)²

(Profiles 1-25)

Profile
No.

Data No.	21	22	23	24	25
1	4.55	4.65	4.56	4.68	4.57
2	6.96	7.08	6.92	7.05	6.95
3	0.54	0.76	0.77	0.77	1.73
4	1.15	1.13	1.36	1.36	1.33
5	1.59	1.98	1.98	1.56	1.51
6	2.28	2.96	3.14	2.43	2.18
7	2.36	2.02	1.83	2.11	2.08
8	1.27	0.68	0.99	1.23	1.20
9	0.95	0.90	0.73	0.92	0.61
10	0.78	0.46	0.32	0.62	1.15
11	0.45	0.31	0.44	0.44	0.03
12					
13					
14					
15					

*Note: Blanks indicate the data approach 0.0

Table

Static Stability $N^2 \times 10^4$ (rad/sec)²
(Profiles 1-25)

DISTRIBUTION LIST

Director 1
Office of Naval Research Branch Office
1030 East Green Street
Pasadena, California 91106

Office of Naval Research 1
San Francisco Area Office
760 Market Street - Room 447
San Francisco, California 94102

Director 1
Office of Naval Research Branch Office
495 Summer Street
Boston, Massachusetts 02210

Director 1
Office of Naval Research Branch Office
536 South Clark Street
Chicago, Illinois 60605

Commanding Officer 8
Office of Naval Research Branch Office
Box 39
FPO New York 09510

Commander 1
Naval Ordnance Laboratory
Acoustics Division
White Oak
Silver Spring, Maryland 20910
Att: Dr. Zaka Slawsky

Office in Charge 1
Annapolis Laboratory
Naval Ship Research and Development Center
Annapolis, Maryland 21402

Defense Documentation Center 10
Cameron Station
Alexandria, Virginia 22314

Superintendent 1
Naval Academy
Annapolis, Maryland 21402

Commanding Officer 1
Naval Intelligence Support Center
4301 Suitland Road
Washington, D.C. 20390
Att: Dr. Johann Martinek
Mr. E. Bissett

Distribution List - 2

Commander 1
Naval Sea Systems Command
Code SEA 03E
Washington, D.C. 20362

Dr. Charles Stutt 1
General Electric Company
P.O. Box 1088
Schenectady, New York 12301

Dr. Harry DeFerrari 1
University of Miami
Rosenstiel School of Marine and
Atmospheric Science
Miami, Florida 33149

Mr. Robert Cunningham 1
Bendix Electronics Center
15825 Roxford Street
Sylmar, California 91342

Dr. Stephen Wolff 1
John Hopkins University
Baltimore, Maryland 21218

Dr. M.A. Basin 1
S.D.P., Inc.
15250 Ventura Blvd., Suite 518
Sherman Oaks, California 91403

Dr. Walter Duing 1
University of Miami
Rosenstiel School of Marine and
Atmospheric Science
Miami, Florida 33149

Dr. David Middleton 1
127 East 91st Street
New York, New York 10028

Dr. Donald W. Tufts 1
University of Rhode Island
Kingston, Rhode Island 02881

Dr. Loren W. Nolte 1
Dept. of Electrical Engineering FT-10
University of Washington
Seattle, Washington 98195

Mr. S.W. Autrey 1
Hughes Aircraft Company
P.O. Box 3310
Fullerton, California 92634

Dr. Thomas W. Ellis 1
Texas Instruments, Inc.
13500 North Central Expressway
Dallas, Texas 75231

Distribution List - 3

Mr. Robert Swarts
Applied Physics Laboratory
University of Washington
1013 N.E. 40th Street
Seattle, Washington 98195

1

Mr. Charles Loda
Institute for Defense Analyses
400 Army-Navy Drive
Arlington, Virginia 22202

1

Mr. Beaumont Buck
Polar Research Laboratory
123 Santa Barbara Avenue
Santa Barbara, California 93101

1

Dr. M. Weinstein
Underwater Systems, Inc.
8121 Georgia Avenue
Silver Spring, Maryland 20910

1

Dr. Thomas G. Kincaid
General Electric Company
P.O. Box 1088
Schenectady, New York 12301

1

Applied Research Laboratories
The University of Texas at Austin
P.O. Box 4029
Austin, Texas 78712
Att: Dr. Lloyd Hampton
Dr. Charles Wood
Dr. T.D. Plemons

4

Woods Hole Oceanographic Institute
Woods Hole, Massachusetts 02543
Att: Dr. Paul McElroy
Mr. R. Porter
Mr. R. Spindel

1

Dr. John Bouyoucos
Hydroacoustics, Inc.
321 Northland Avenue
P.O. Box 3818
Rochester, New York 14610

1

Systems Control, Inc.
260 Sheridan Avenue
Palo Alto, California 94306
Att: Mr. Robert Baron

1

Dr. David Hyde
Special Assistant (Electronics)
Office of the Assistant
Secretary of the Navy
R&D Pentagon
Washington, D.C. 20350

1

Distribution List - 4

CDR. Harry C. Furminger, USN
Commanding Officer
U.S. Naval Facility
FPO, New York 09556

Dr. Victor C. Anderson
Marine Physical Laboratory
Scripps Institution of Oceanography
University of California
La Jolla, Calif. 92037

1

Mr. Robert Swartz
Applied Physics Laboratory
University of Washington
1013 N.E. 40th Street
Seattle, Washington 98195

Mr. Charles Loda
Institute for Defense Analysis
400 Army-Navy Drive
Alexandria, Virginia 22304

Mr. Raymond Buck
Polar Research Laboratory
123 Santa Barbara Avenue
Santa Barbara, California 93101

Dr. H. Weinstein
Underwater Systems, Inc.
3111 Georgia Avenue
Silver Spring, Maryland 20910

Dr. Thomas C. Kincaid
General Electric Company
P.O. Box 1084
Schenectady, New York 12301

Applied Research Laboratories
The University of Texas at Austin
P.O. Box 4029
Austin, Texas 78712
Attn: Dr. Lloyd Hampton
Dr. Charles Wood
Dr. T.D. Williams

Woods Hole Oceanographic Institute
Woods Hole, Massachusetts 02543
Attn: Dr. Paul McElroy
Mr. R. Farber
Mr. R. Spindler

Dr. John Bonycastle
Hydroacoustics, Inc.
211 Northland Avenue
P.O. Box 3818
Beverly, New York 14610

Systems Control, Inc.
280 Sheridan Avenue
Palo Alto, California 94306
Attn: Mr. Robert Baron

Dr. David Hyde
Special Assistant (Electronics)
Office of the Assistant
Secretary of the Navy
NAB Building
Washington, D.C. 20350

UNCLASSIFIED

SECURITY CLASSIFICATION OF THIS PAGE (When Data Entered)

REPORT DOCUMENTATION PAGE		READ INSTRUCTIONS BEFORE COMPLETING FORM
1. REPORT NUMBER (14) IAR-78001	2. GOVT ACCESSION NO.	3. RECIPIENT'S CATALOG NUMBER
4. TITLE (and Subtitle) (6) BEAR BUOY: Analyses of Acquired Temperature Data,	5. TYPE OF REPORT & PERIOD COVERED (9) Final Report, Jul 1978	6. PERFORMING ORG. REPORT NUMBER 8 Mar-78 Jul 78
7. AUTHOR (18) Kenneth L. Echternacht	8. CONTRACT OR GRANT NUMBER(s) (15) N00014-74-C-0229	
9. PERFORMING ORGANIZATION NAME AND ADDRESS Institute for Acoustical Research 615 S.W. 2nd Ave. Miami, Fla. 33130	10. PROGRAM ELEMENT, PROJECT, TASK AREA & WORK UNIT NUMBERS	
11. CONTROLLING OFFICE NAME AND ADDRESS Procuring Contracting Officer Office of Naval Research, Dept. of the Navy, Arlington, Va. 22217	12. REPORT DATE (11) July 1978	13. NUMBER OF PAGES 51
14. MONITORING AGENCY NAME & ADDRESS (if different from Controlling Office) Office of Naval Research Resident Rep. Columbia University Lamont Doherty Geological Observatory Torrey Cliff, Palisades, N.Y. 10913	15. SECURITY CLASS. (of this report) Unclassified	15a. DECLASSIFICATION/DOWNGRADING SCHEDULE
16. DISTRIBUTION STATEMENT (of this Report) "Reproduction in whole or in part is permitted for any purpose of the U.S. Government", Distribution of the Document is Unlimited. (12) 54 p.		
17. DISTRIBUTION STATEMENT (of the abstract entered in Block 20, if different from Report)		
18. SUPPLEMENTARY NOTES		
19. KEY WORDS (Continue on reverse side if necessary and identify by block number) Buoy measurements Temperature profiles Static stability profiles Sound velocity profiles Density profiles		
20. ABSTRACT (Continue on reverse side if necessary and identify by block number) This study examines the temporal variation in temperature at several levels from near surface to below the thermocline - a depth of approximately 1900 m. The time series were collected over a 51 day period from 16 February through 6 April 1976 from an area approximately 40 Km northeast of the island of Eleuthera, Bahamas. The study also includes an examination of the temporal and depth changes		

DD FORM 1 JAN 73 1473

EDITION OF 1 NOV 63 IS OBSOLETE
S/N 0102-014-6601

UNCLASSIFIED

SECURITY CLASSIFICATION OF THIS PAGE (When Data Entered)

408141

CONT

UNCLASSIFIED

SECURITY CLASSIFICATION OF THIS PAGE(When Data Entered)

cont

in the density and Brunt-Vaisala frequency over the period of the record. These changes are discussed in terms of observed changes in the level of activity of the internal tides.



UNCLASSIFIED

UNCLASSIFIED

SECURITY CLASSIFICATION OF THIS PAGE(When Data Entered)